3

Temperature, concentration and cholesterol dependent translocation of L- and D-octaarginine across the plasma and nuclear membrane of CD34+ leukaemia cells

Marjan M. Fretz, Neal A. Penning, Saly Al-Taei, Shiroh Futaki, Toshihide Takeuchi, Ikuhiko Nakase, Gert Storm and Arwyn T. Jones

Accepted for publication in the Biochemical Journal

ABSTRACT

Delineating the mechanisms by which cell penetrating peptides such as HIV-TAT peptide, oligoarginines and penetratin gain access to cells has recently received intense scrutiny. Heightened interest in these entities stems from their abilities to enhance cellular delivery of associated macromolecules such as genes and proteins, suggesting they may have widespread applications as drug delivery vectors. Proposed uptake mechanisms include energy-independent plasma membrane translocation and energy-dependent vesicular uptake and internalisation through endocytic pathways. Here we investigated the effects of temperature, peptide concentration and plasma membrane cholesterol levels on the uptake of a model cell penetrating peptide, octaarginine (L-R8) and its D-enantiomer (D-R8) in $CD34^+$ leukaemia cells. We find that at 4-12˚C, L-R8 uniformly labels the cytoplasm and nucleus but in cells incubated with D-R8 there is additional labeling of the nucleolus, that is still prominent at 30˚C incubations. At temperatures between 12-30˚C, the peptides are also localised to endocytic vesicles, that consequently appear as the only labeled structures in cells incubated at 37˚C. Small increases in the extracellular peptide concentration in 37˚C incubations result in a dramatic increase in the fraction of the peptide that is localised to the cytosol and promoted the binding of D-R8 to the nucleolus. Enhanced labeling of the cytosol, nucleus and nucleolus was also achieved by extraction of plasma membrane cholesterol with methyl-ß-cyclodextrin. The data argues for two, temperature-dependent, uptake mechanism for these peptides and for the existence of a threshold concentration for endocytic uptake that when exceeded promotes direct translocation across the plasma membrane.

INTRODUCTION

The scientific literature describes an ever-increasing library of peptides that mediate the lysis of biological membranes or have capacities to translocate through these structures in the absence of increasing porosity to other molecules. An example of the former is mellitin, but recently more attention has been focused on cell penetrating peptides (CPP), also called protein transduction domains, such as the TAT peptide from the HIV-TAT protein and penetratin from the *Drosophila melanogaster* homeobox protein Antennapedia (1). A particular interest in these CPPs derives from their abilities in *vitro* and in *vivo* to overcome cellular barriers such as the plasma membrane, and deliver therapeutic macromolecular cargo, including genes and proteins, into cells (2-5)

A prerequisite to efficient utilization of these peptides as delivery vectors is an enhanced understanding of (a) their interaction with cell surface components - proteins, carbohydrate, lipids, (b) their mechanism of uptake - endocytosis, direct translocation, and (c) their intracellular fate - delivery to lysosomes, dynamics in the cytosol and delivery to the nucleus. Since the discovery that a number of CPP effects is due to fixation artifacts (6, 7), the concept that cellular entry was via direct plasma membrane translocation has been somewhat superceded by models showing that entry is via some form of endocytic route, and that translocation occurs across membranes of the endo-lysosomal system or even the endoplasmic reticulum (7-11). These studies mostly relate to microscopical and flow cytometry analysis of the peptides as fluorescent conjugates, their attachment to larger cargo will undoubtedly affect their interactions with cells and their translocation capacities (12, 13).

Studies from our laboratories and others, using oligoarginine (R7-R9) and HIV-TAT peptides have shown, however, that despite the use of stringent methods to remove plasma membrane associated peptides with trypsin and heparin, a significant fraction enters cells and nucleus at 4˚C (11, 12, 14, 15). Uptake of fluorescent HIV-TAT and octaarginine (R8) peptides in the nonadherent leukaemic KG1a cell line was not inhibited by placing the cells on ice, but the labeling was diffusely localised throughout the cells compared with only vesicular labeling at 37˚C (11). Similar observations have been demonstrated in a number of adherent cell lines (12, 14, 15). Other studies in HUVEC and macrophages show that 4˚C incubations inhibited uptake by ~75% compared with incubations performed at 37˚C (10), and claims also exist for no uptake at 4˚C (9). Though there is disparity over the extent of cellular association at 4˚C there is general uniformity with respect to the fact that a significant fraction enters cells in the absence of endocytic mechanisms. Recent data also suggests that R8 was able to enhance delivery of liposomes at both 37 and 4˚C (16).

Model membrane systems have also been utilised to investigate the translocation capacities of these peptides and as expected this process is dependent on peptide sequence and the lipid composition of the membranes (17-21). These studies have allowed for proposals for the mechanism by which the peptides interact with and traverse membrane systems and

favored models suggest they are driven via a potential difference following membrane destabilization, that they induce the formation of inverted micelles or that they themselves mediate pore formation.

To further investigate the effects of temperature on cellular peptide uptake, we have performed quantitative and qualitative analysis with the model CPP R8-Alexa488 and its D-enantiomer in a leukaemia cell line. We find that peptide localization is sensitive to cholesterol sequestration, peptide concentration, and the incubation temperature, such that a reduction in endocytosis at low temperatures is paralleled by an increase in peptide translocation through the plasma membrane.

EXPERIMENTAL METHODS

Materials

Maleimide-C5-Alexa488 and Alexa488-transferrin (Alexa488-Tf) were from Invitrogen (Paisley, UK), DRAQ5 dye was a kind gift from Biostatus (Shepshed, UK). N-acetylcysteine and methyl-β-cyclodextrin (MβCD) were purchased from Sigma (Poole, UK).

Peptide synthesis

The two peptides used in this study were generated by 9-fluorenylmethyloxycarbonyl (Fmoc) solid phase synthesis and labeled at the C-terminal cysteine using Maleimide-C5-Alexa488 sodium salt as fluorescent dye as previously described (11). Purification and characterization was achieved by HPLC and MALDI-TOF mass spectrometry respectively. The final peptide products were L-R8-Alexa488 containing naturally abundant L-arginine [NH_2-$(Arg)_8$-Gly-Cys(Alexa 488)-amide] or D-R8-Alexa488 [NH_2-$(_D$-$Arg)_8$-Gly-Cys(Alexa 488)-amide].

Cell culture

The haematopoietic cell line KG1a was maintained at confluency of 0.5 – 2 x 10^6 cells/ml in RMPI 1640 supplemented with 10% fetal calf serum, 100 IU/ml penicillin and 100 µg/ml streptomycin at 37°C with 5% CO_2 in humidified air. All cell culture reagents were obtained from Invitrogen (Paisley, UK).

Fluorescence microscopy

KG1a cells (0.5 x 10^6) were washed once with complete RPMI 1640 medium (CM) and equilibrated for 15 min in complete medium set to temperatures 4 (ice), 12, 19, 30 and 37˚C. The medium was then replaced by 200 µl fresh equilibrated complete medium containing 2-10 µM of L-or D-R8-Alexa488 or 100 nM Alexa488-Tf and incubated at these temperatures for 1 h. The cells were washed twice with ice-cold PBS and once with serum free RMPI 1640 medium without phenol red, serum or antibiotics (imaging medium), and resuspended in approximately 20 µl of imaging medium. In some experiments, DRAQ5 dye was used to label the nucleus and this was added at room temperature (10 µM) for 3 min prior to the last washing step.

Finally, 2 µl of the cell suspension was transferred to a well of a 10-well multispot microscope slide (Hendley, Essex, UK), that was then layered with a coverslip. Live cells were then immediately analysed by fluorescent microscopy. Wide field fluorescent images were obtained on a Leica DMIRB inverted fluorescent microscope equipped with a 63x oil immersion objective and QIMAGING RETIGA 1300 camera (Burnaby, BC, Canada). The acquired images were processed with Improvision Openlab 5.0.2 software (Coventry, U.K).

Confocal microscopy was performed on a Leica TCS-SP2 RS confocal laser-scanning microscope equipped with an Ar and HeNe laser and a 63x oil immersion objective. Leica LCS Lite software was used to merge and stack individual confocal sections through the z-axis to generate maximum projection images.
In one designated experiment, cells were incubated with 2 μM L-R8-Alexa488 for 1 h and following washing were fixed in 3% (w/v) paraformaldehyde for 15 min prior to further washes and analysis by fluorescence microscopy.

Flow cytometry
KG1a cells (0.5 x 10^6) were equilibrated and incubated for 1 h with 2 μM L- or D-R8-Alexa488 at different temperatures as described above. Alternatively, cells were washed in ice cold CM and incubated with 0.25 – 5 μM L- or D-R8-Alexa488 for 1 h at 4°C. The cells were washed three times with ice-cold PBS, resuspended in 200 μl of PBS and Alexa488 fluorescence was measured using a Becton & Dickinson FACScalibur analyser. In some experiments, following peptide incubation, the cells were washed once with PBS, incubated with 0.25 mg/ml trypsin solution for 5 min at 37°C, washed once with ice-cold PBS and finally twice with PBS containing 14 μg/ml heparin. Live cells were gated on Forward Scatter and Side Scatter and 10,000 viable cells were analysed.

Analysis of binding and uptake of activated and inactivated Alexa488-C5-maleimide
Unconjugated (activated) Alexa488-C5-maleimide was dissolved in methanol to a concentration of 1.78 mM. For inactivation, 375 μl of the solution was incubated at room temperature for 4 h with a 4-fold molar excess of N-acetylcysteine (10 mg/ml in PBS). The solution was then stored at -20°C until use. For cell studies, KG1a cells (0.5 x 10^6) were equilibrated on ice or at 37˚C, washed and further incubated on ice or at 37˚C in CM containing 2 μM activated or inactivated dye. Finally the cells were washed two times with imaging medium and analysed, as described, by fluorescent microscopy.

Binding and uptake of peptides and transferrin by MβCD-treated cells
MβCD was dissolved in PBS to 76 mM and diluted to 5 mM in serum free medium (SFM). KG1a cells (0.5 x 10^6) were washed once with SFM, resuspended in 200 μl SFM containing 5 mM MβCD and incubated under tissue culture conditions for 30 min. Control cells were treated as above but in the absence of MβCD. The cells were then washed with SFM and incubated for 1 h at 37˚C with 2 μM L- or D-R8-Alexa488 or 100 nM Tf-Alexa488 in SFM. The cells were washed twice with SFM, resuspended in imaging medium and analysed by fluorescence microscopy.

Cell viability studies

KG1a cells (4 x 10^4 cells/well in a total volume of 200 µl) were seeded in 96-well plates and incubated with 0 - 50 µM L- or D-R8-Alexa488 for 24 h under tissue culture conditions. Cell viability was then assessed using MTT assays (22). Briefly, 20 µl MTT, 5.5 mg/ml in SFM, was directly added to each well giving a final concentration of 0.5 mg/ml. The cells were then incubated for 4 h under tissue culture conditions. The plates were centrifuged at 1000 x *g* for 5 min prior to removing the supernatant and then adding 100 µl DMSO. The samples were finally incubated at 37°C for 30 min prior to quantifying the absorbance at 550 nm.

RESULTS

Comparative analysis of the subcellular distribution of L- and D-R8-Alexa488.

We previously reported on the distinct labeling patterns of L-R8-Alexa488 in the $CD34^+$ leukaemic KG1a cell line when incubations were performed either on ice (here referred to as 4˚C) or at 37˚C (11). As shown in Figure 1A, confocal microscopy of cells incubated for 1 h at 4˚C with 2 µM L-R8-Alexa488 reveals the peptide to be localised throughout the cell including the nucleus and this compares with vesicular labeling only, when identical experiments are performed at 37˚C (Figure 1C).

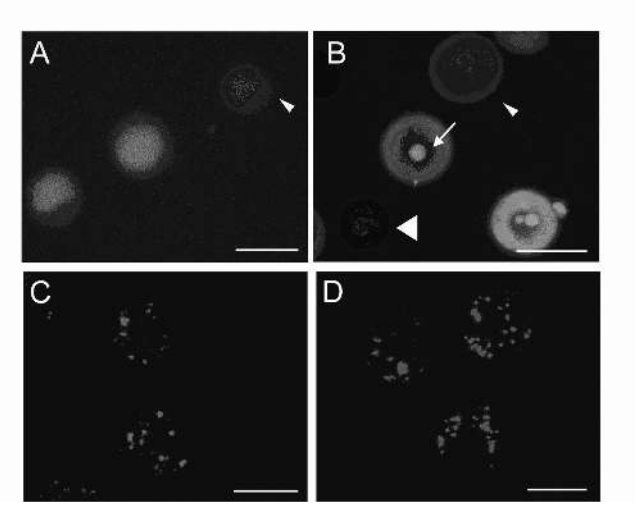

Figure 1. Cellular distribution of L- and D-R8-Alexa488 in KG1a cells at 4 and 37°C (A-D) KG1a cells were incubated for 1 h with 2 µM L- (A, C) or D-R8-Alexa488 (B, D) at either 4°C (A-B) or 37°C (C-D), prior to analysis by confocal microscopy. Shown are maximum projections of 35 z-stacks (~ 500 nm/ and 2 to 4 s/section) for each condition. A and B were also labeled with DRAQ5 dye as described in experimental. Arrows in B indicate peptide labeling of nucleolus, small arrowhead show a cell showing low peptide labeling, large arrowhead shows a cell with undetectable levels of peptide fluorescence. Scale bars 10 µm.

Our ability to label the nucleus of these live cells with the DRAQ5 probe also supports our previous observations showing heterogeneity with respect to the intensity of peptide labeling when peptide incubations are performed at this temperature (11). To obtain these images we captured multiple sections through the z-axis and then overlaid the data to create a single merged maximum projection image.

We performed identical experiments with the D-enantiomer of R8, and similar to the L form, the peptide localises to vesicles at 37˚C (Figure 1D). When the cells were incubated with D-R8-Alexa488 at 4˚C, we observed diffuse labeling that was less apparent in the

nucleus but much more prominent in the nucleolus (Figure 1B). This image also highlights the heterogeneity of peptide labeling at 4˚C, from high to undetectable.
In order to refute the possibility that these effects are caused by extracellular protease-mediated degradation of the peptide, with resulting release and internalisation of free fluorophore, we initially incubated the cells at 4 or 37˚C with the activated Alexa488 maleimide dye that is used to link to the terminal cysteine of the peptide (Figure 2A).

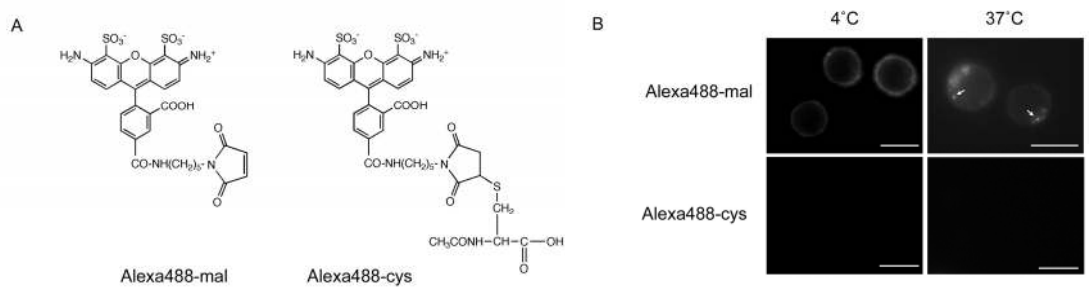

Figure 2 Cellular distribution of activated and inactivated Alexa488-C5-maleimide
(A) Chemical structures of activated (Alexa488-mal) and inactivated Alexa488-C5-maleimide (Alexa488-cys), following its conjugation to N-acetylcysteine. (B) Cellular distribution of Alexa488-mal and Alexa488-cys. KG1a cells were incubated with 2 μM label for 1 h at 4 or 37˚C prior to washing and analysis by fluorescence microscopy. Arrows depict vesicular labeling that was only observed with Alexa488-mal at 37˚C. Scale bars 10 μm.

At 4˚C the fluorescence of this compound was confined to the plasma membrane and when identical experiments were performed at 37˚C, intracellular vesicles were also labeled (Figure 2B). However, compared to experiments performed with the equivalent concentrations of Alexa488-R8 (Figure 1), much higher exposure times were required to observe these structures. This suggested that at both temperatures, the activated dye was conjugating to plasma membrane sulfhydryl groups and that these conjugates remained on this structure in the absence of endocytosis at 4˚C but were internalised at 37˚C. We therefore inactivated the maleimide functional group with N-acetylcysteine and observed that even the relatively high exposure times utilized to see the activated dye at 37˚C were not sufficient to label the cells at either temperature (Figure 2B). Thus the fluorescence observed in Figure 1 was a product of R8-mediated delivery to endosomes at 37˚C or to the cytosol, nucleus and nucleolus at 4˚C. We performed identical experiments with a control peptide NH_2-(Gly-Ser)$_4$-Gly-Cys(Alexa 488)-amide and at 2 μM this was undetectable in cells using fluorescence microscopy (data not shown).

Effects of temperature on subcellular distribution and cellular fluorescence profiles for L- and D-R8-Alexa488.

Similar microscopy experiments were then performed with L- and D-R8-Alexa488 at temperatures between 4 and 37˚C. Figure 3 shows that L-R8-Alexa488 diffusely labels the entire cell when incubations are performed at ≤ 19˚C, but at higher temperatures to 30˚C, the diffuse fluorescence is accompanied by vesicular labeling. In cells incubated with the D-R8 peptide there was similar but additional nucleolar labeling at all temperatures ≤ 30˚C; at 37˚C cellular labeling of both peptides was confined to vesicular structures. We also performed the same experiments with Alexa488-Transferrin (Alexa488-Tf), that at 4˚C is expected to only bind the transferrin receptor at the plasma membrane but not be internalised, and at higher temperatures will be endocytosed into clathrin coated vesicles and endosomes (23, 24). As expected, this protein labeled only the plasma membrane at ≤12˚C, but at higher temperatures, plasma membrane labeling was accompanied by vesicular labeling that increased in intensity as the temperature was increased to 37˚C. Thus, these octaarginine-based peptides behaved quite differently from each other and from Tf when they were incubated with cells at temperatures ≤30˚C. The data also suggest that unlike Tf, the peptides have at least two independent, but temperature-dependent uptake mechanisms. Similar differences in cellular distribution of peptides Tat P59W, R7 and R7W, were also noted in adherent cells when incubations are performed at 4˚C or 37˚C (12, 15), thus suggesting this differential labeling is not a feature unique to these leukaemia cells. We previously showed using flow cytometry that cellular fluorescence profiles of cells incubated with R8 at 4˚C differ from those incubated at 37˚C (11, 14).

We therefore performed flow cytometry analysis with cells incubated with 2 μM L- and D-R8-Alexa488 at the same selected temperatures between 4 and 37˚C. The results shown in Figure 4 show clear temperature dependent profiles, but the L and D forms gave very similar results. Two peaks were observed for both peptides after 4 to 12˚C incubations but at 19˚C the lower peak is much more apparent with a concomitant broadening of the high peak. Only one peak is observed for both peptides when incubated with cells at 30 to 37˚C.

Again, Alexa488-Tf was used for comparative analysis, and only one fluorescence peak, with the expected increasing intensity with increasing concentration, was observed at all temperatures (Figure 4). For this ligand, the data allows for easy quantification of cell-associated fluorescence, but this is not the case for quantification of cell-associated L- or D-R8-Alexa488 at <30˚C. This is why the profiles are shown here rather than just the geometric mean values. Interestingly, previous studies in Jurkat T-cells also showed two peaks of fluorescence, but the cells were incubated with a much higher concentration (12.5 μM) of R9 at 25 ˚C (25).

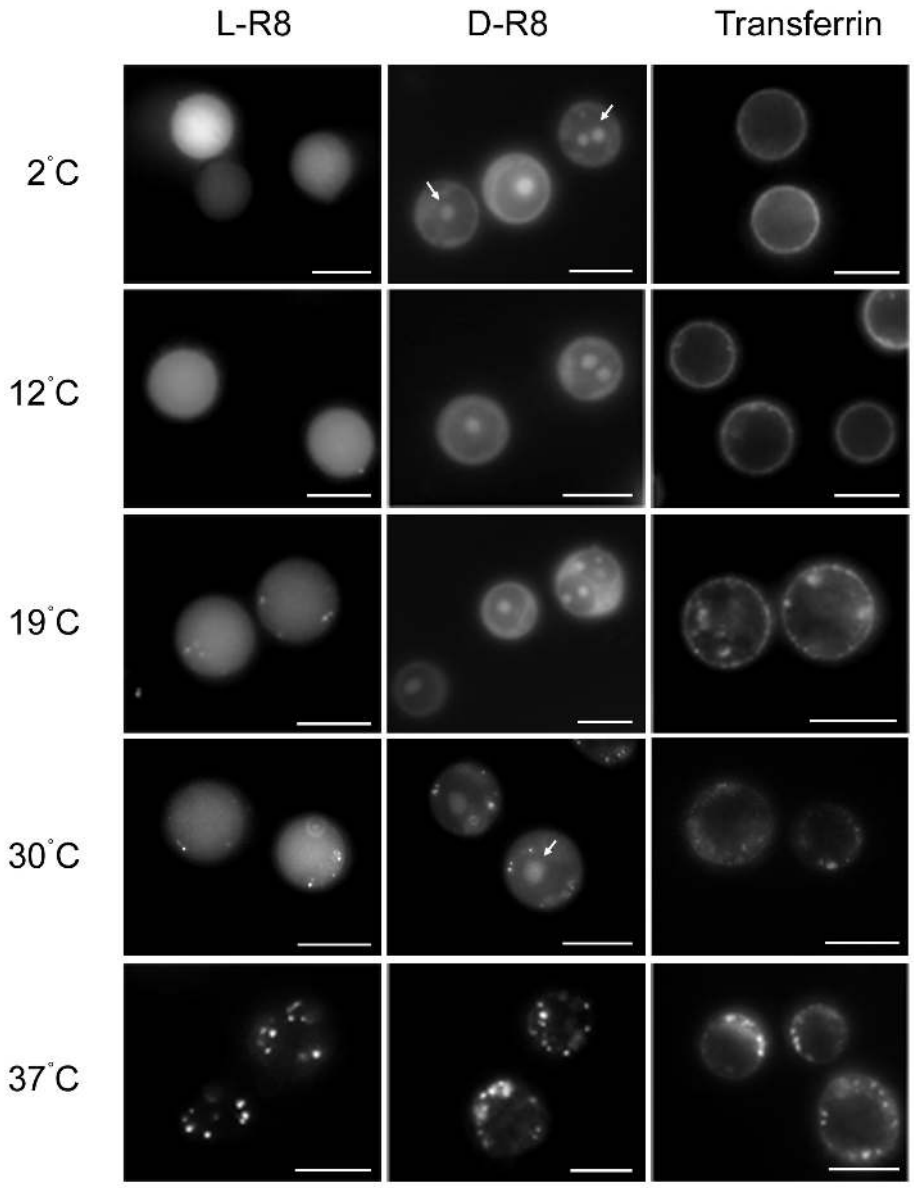

Figure 3. Temperature-dependent cellular distribution of R8-Alexa488 peptides and Alexa488-Tf. KG1a cells were incubated at 4 - 37˚C for 1 h with 2 µM L- or D-R8-Alexa488 or 100 nM Alexa488-Tf prior to washing and analysis by fluorescence microscopy. Arrows depict labeling of the nucleolus that is unique to D-R8-Alexa488 at ≤30 ˚C. Scale bars 10 µm.

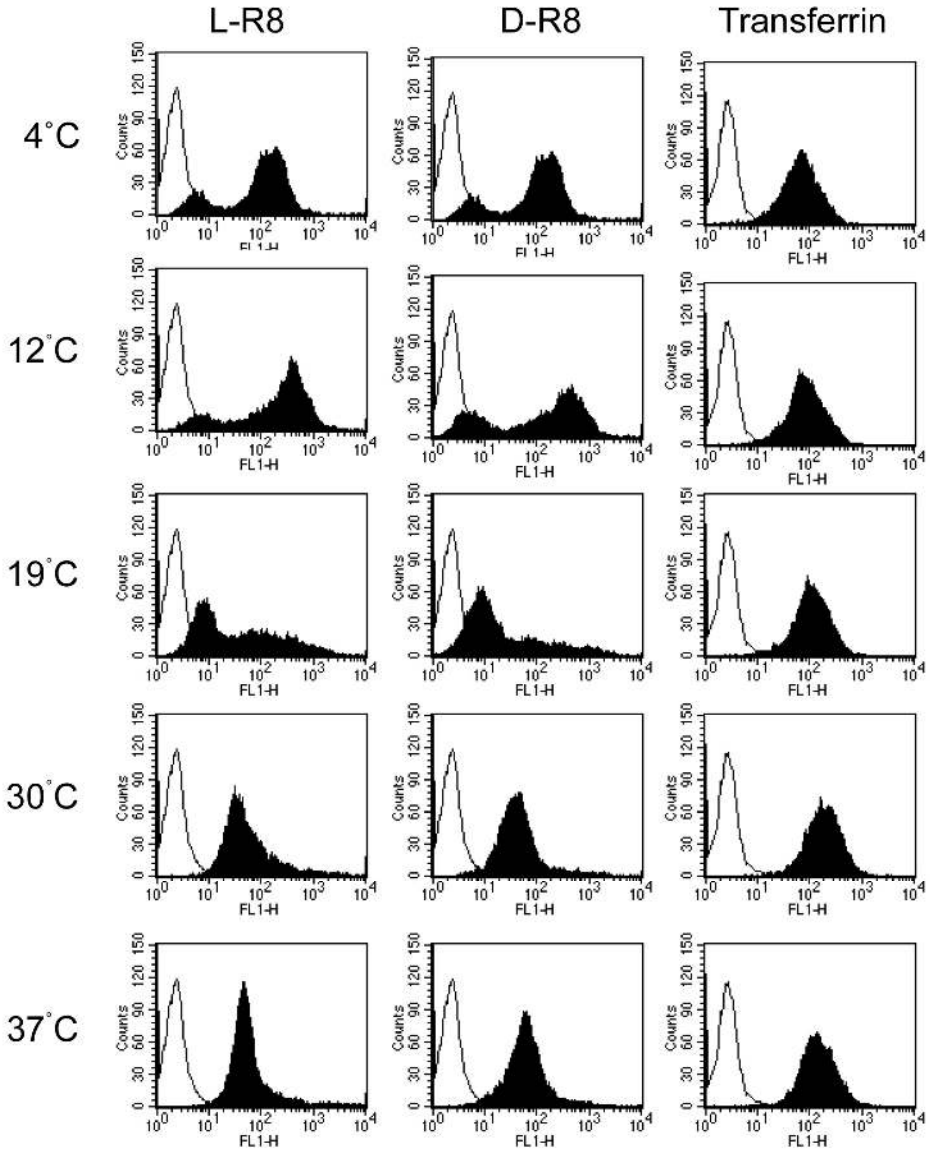

Figure 4. Temperature-dependent cellular fluorescence profiles for R8-Alexa488 peptides and Alexa488-Tf. KG1a cells were incubated at 4 - 37˚C for 1 h with 2 μM L- or D-R8-Alexa488 or 100 nM Alexa488-Tf prior to washing and analysis by flow cytometry. Unfilled peaks represent untreated cells

In conclusion, the data from this section suggest that endocytosis of peptides and transferrin occurs at a reasonably uniform rate throughout the cell population but that differences exist with respect to the capacity of the cells to associate with the peptides at temperatures < 37˚C.

Effects of concentration on subcellular distribution and cellular fluorescence profiles for L- and D-R8-Alexa488.

We then investigated whether the cellular fluorescence profiles that we observed at 4˚C were sensitive to the concentration of the peptides in the medium. Cells were incubated with 0.25 – 5 µM peptide for 1 h prior to washing and immediate analysis by flow cytometry or, following the peptide incubations, they were further treated with trypsin and washed with heparin solutions. These additional steps have been shown to reduce plasma membrane labeling that contributes significantly to the fluorescence values in adherent cells (7).

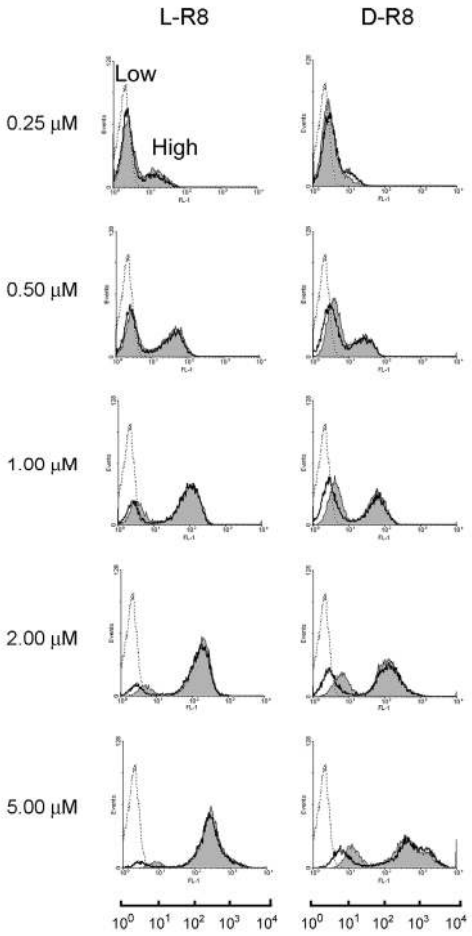

Figure 5. Concentration-dependent cellular fluorescence profiles for R8-Alexa488 peptides. KG1a cells were incubated for 1 h with 0.25 to 5.0 µM L- or D-R8-Alexa488 at 4°C. The cells were then washed and either immediately analysed by flow cytometry (filled grey) or were further treated with trypsin and heparin prior to analysis (unfilled peaks). Dotted lines represent untreated cells. In all experiments performed at 4˚C, two peaks of fluorescence of varying intensities were obtained, and designated Low and High. The geometric mean values of the two designated peaks were calculated for all conditions and these contributed with repeat experiments to generate Table 1.

The data in Figure 5 shows that L- and D-R8-Alexa488 generated two peaks of fluorescence at all concentrations, and irrespective of whether the cells were further subjected to trypsin and heparin treatment. These were designated Low and High and the mean intensity of both generally increased as the peptide concentration was increased; this was accompanied by an increase in the fraction of cells that appeared in the High peak. Trypsinisation appeared to have minimal effects on the fluorescent profiles but at >2 μM there was a visible reduction in the geometric mean of the low peaks. To analyse this further, the geometric means of the separate peaks at all studied concentrations were quantified and the results in Table 1 demonstrate that the fluorescence of the low peaks are significantly reduced ($P < 0.05$) by trypsin/heparin treatment at concentrations ≥ 0.5 μM for L-R8 or ≥ 1 μM for D-R8. However there was no significant decrease in the fluorescence of the high peak when the peptide concentration was ≥ 0.5 μM, and even at 0.25 μM peptide concentration, ≥ 75% of the fluorescence in the high peak fraction was insensitive to trypsin/heparin treatment.

Table 1 Analysis of fluorescence peaks obtained from incubating cells with increasing concentrations of R8-Alexa488 peptides. KG1a cells were incubated with 0.25 – 5.0 μM L- or D-R8-Alexa488 for 1 h at 4 °C. The cells were then washed and either immediately analysed by flow cytometry (PBS) or further treated with trypsin and heparin prior to analysis (trypsin/heparin). Two peaks of fluorescence were observed and designated Low and High (Figure 5). Shown are the geometric mean values for the Low and High peaks for all depicted concentrations. Data represent mean and SD from two individual experiments performed in duplicate. Statistical analysis for comparing the geometric means of untreated versus treated fluorescence cells was performed using students t-test. (*) Decreased relative to PBS control $P < 0.05$

L-R8

Peptide concentration (μM)	Low		High	
	PBS	Trypsin/heparin	PBS	Trypsin/heparin
0.25	2.76 ± 0.14	2.78 ± 0.45	17.20 ± 0.45	16.10* ± 0.26
0.50	3.12 ± 0.13	2.94 ± 0.12	39.99 ± 3.27	37.87 ± 2.35
1.00	3.89 ± 0.23	3.16* ± 0.22	98.88 ± 4.60	93.64 ± 2.74
2.00	4.78 ± 0.28	3.51* ± 0.19	175.14 ± 10.61	165.90 ± 14.05
5.00	9.44 ± 1.21	4.69* ± 0.47	357.73 ± 62.42	338.55 ± 46.47

D-R8

Peptide concentration (μM)	Low		High	
	PBS	Trypsin/heparin	PBS	Trypsin/heparin
0.25	3.18 ± 0.12	2.94 ± 0.19	15.73 ± 1.27	12.46* ± 0.57
0.50	4.09 ± 0.18	3.07* ± 0.05	28.71 ± 5.20	30.77 ± 4.56
1.00	4.80 ± 0.51	3.17* ± 0.17	83.14 ± 19.10	76.78 ± 17.98
2.00	6.07 ± 0.17	3.82* ± 0.28	147. 86 ± 16.75	155.025 ± 13.61
5.00	11.83 ± 1.69	6.18* ± 1.05	430.48 ± 63.94	521.81 ± 105.11

We do not currently have an explanation as to why a particular cell should fall into the Low or High peak population. It is conceivable that the low peak represents cells with the peptide located within the extracellular matrix of the plasma membrane or even embedded in the lipid bilayer and that this fraction is only partially sensitive to trypsin and heparin treatment. When cells were incubated for 1 h at 4˚C with L-R8-Alexa488, washed and then incubated for a further 1 hour at 4˚C or at 37˚C, there was no significant effect on cellular fluorescence profiles or low and high peak values (data not shown).

The possibility also exists that the loss of the low peak at higher peptide concentrations is a result of fluorescence quenching and that for L-R8, fluorescence could be further diminished by proteolysis. This is however unlikely as the intensity of the low peaks is enhanced with increasing peptide concentrations but do not increase in intensity upon trypsinisation and heparin washing and neither do they shift to baseline levels. Parallel experiments of peptide association versus cell cycle status may help define characteristics that predispose the cells to having different capacities to associate with or internalise these peptides.

Fluorescence microscopy was then utilised to determine whether increasing the peptide concentration from our standard 1 to 2 μM affected the subcellular labeling pattern when incubations were performed at 37˚C. Cells were therefore incubated with 2 to 10 μM peptide for 1 h, washed and then analysed.

Figure 6A shows that increasing the concentration from 2 to only 5 μM resulted in a dramatic increase in the fraction of the peptide that was localised to the cytosol. Vesicular labeling was still evident at this higher concentration, up to 10 μM, but this was somewhat masked by the strong diffuse labeling. In cells incubated with 10 μM D-R8-Alexa488 the nucleolus was also prominently labeled but L-R8-Alexa488 failed to label these structures even at these higher concentrations. In all our experiments we were unable to observe the presence of L-R8-Alexa488 in the nucleolus but clear nucleolar labeling was observed when cells, incubated with 2 μM peptide at 4 or 37˚C, were fixed with paraformaldehyde prior to microscopical analysis (Figure 6B and data not shown).

These data strongly suggest that endocytosis as an uptake mechanism, and visible by fluorescence microscopy, is only dominant to a specific peptide concentration. At levels higher than this threshold, the peptide also enters cells by an alternative mechanism. It is highly unlikely that this very strong cytoplasmic labeling at 5 to 10 μM is caused by endocytosis and then translocation from the endo-lysosomal system as similar data was obtained when the peptide incubations were reduced to 10 min (Figure 6C).

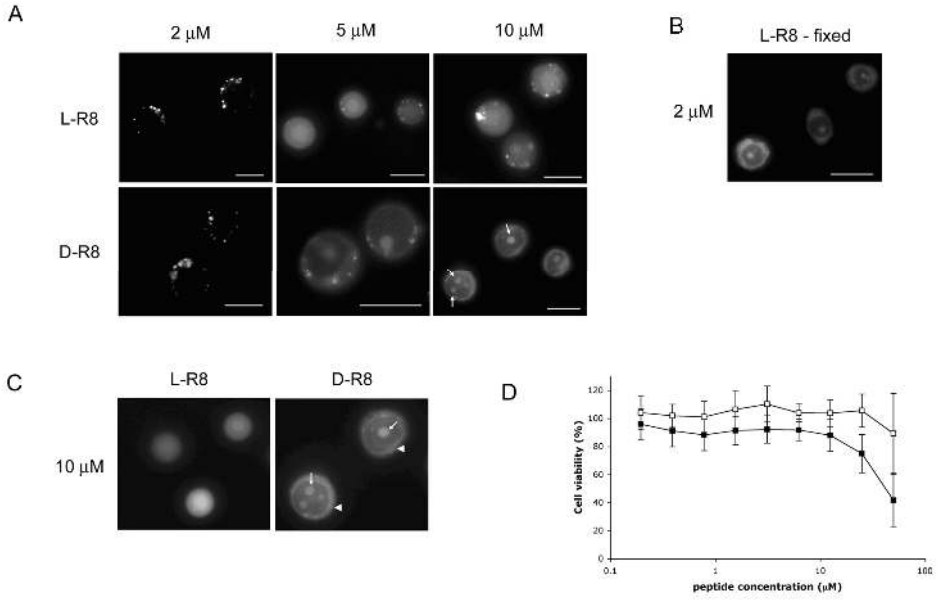

Figure 6. Concentration-dependent cellular distribution and toxicity profiles for R8-Alexa488 peptides (**A**) KG1a cells were incubated with 2, 5 or 10 μM L- or D-R8-Alexa488 for 1 h at 37°C prior to washing and analysis by fluorescence microscopy. Arrows depict labeling of the nucleolus; scale bars 10 μm. (**B**) KG1a cells were incubated with 2 μM L-R8-Alexa488 for 1 h at 37 °C. After washing, cells were fixed with paraformaldehyde prior to analysis by fluorescence microscopy. (**C**) KG1a cells were incubated with 10 μM L- or D-R8-Alexa488 for 10 min at 37°C prior to washing and analysis by fluorescence microscopy. Arrows depict labeling of the nucleolus, arrowheads show faint vesicular labeling **(D)** Cell viability of KG1a cells in the presence of increasing concentrations of R8-Alexa488 peptides. KG1a cells were incubated with 0 - 50 μM L-R8-Alexa488 (open squares) or D-R8-Alexa488 (filled squares) for 24 h prior to performing MTT assays. Cell viability is expressed as the percentage of viable cells relative to untreated controls. Data are from a two experiments performed in quadruplicate and values represent mean ± SD.

Vesicular labeling in these shorter incubations was however less pronounced. Equally it is unlikely that at low peptide concentrations at 37˚C that translocation from cytosol to endosomes and lysosomes is significant, as incubations performed at 4˚C in the presence of peptide followed by 37˚C incubations without peptides, had no effects on the pattern of labeling (Data not shown).

At concentrations ≥ 5 μM, it is conceivable that some of the observed effects were due to peptide induced membrane damage and cytotoxicity. Parallel experiments were therefore performed in cells incubated with 10 μM L- or D-R8-Alexa488 and propidium iodide (PI), that would only be expected to enter dead or leaky cells. There was no increase in PI labeled cells under these conditions (data not shown) and longer 24 h cell viability assays demonstrated that D and L peptides lacked significant toxicity up to 12.5 μM (Figure 6D).

The majority of studies investigating the uptake mechanisms of CPPs have also utilised peptide concentrations between 0.5 to 10 μM, however the universality of these effects with respects to other types of cells remains to be determined. There is likely to be different threshold concentrations for different cell lines as each will have their unique repertoire of plasma membrane lipids, proteins, and their associated carbohydrates. These may all affect the degree of peptide association with molecules protruding from the plasma membrane and/or with molecules localized within the bilayer itself.

Effects of cholesterol depletion on subcellular distribution of L- and D-R8-Alexa4 As translocation across membranes was occurring at higher concentrations of peptide, we investigated whether this process could be promoted at lower concentrations by perturbing the organisation of the plasma membrane. For this, we depleted plasma membrane cholesterol using a standard method employing the cholesterol sequestering agent methyl-ß-cyclodextrin (MßCD) (26). Cells were pretreated with 5 mM MßCD for 30 min prior to addition of 2 μM L- or D-R8-Alexa488 for 1 h at 37˚C and immediate analysis by fluorescence microscopy. MßCD treated cells had strong diffuse labeling of the cytoplasm and nucleus with very little evidence of vesicular uptake; consistent with our previous experiments, nucleolar labeling was unique to the D-form.

Very different results were obtained when parallel experiments were performed with Alexa488-Tf, and here, cholesterol sequestration completely inhibited vesicular uptake and only the plasma membrane was labeled. MßCD was previously shown to significantly inhibit uptake of TAT peptide (9) and penetratin in a number of cell lines (27), suggesting that uptake is occurring via plasma membrane domains called rafts. These are enriched in cholesterol (28), and MßCD is often used to discriminate between uptake via clathrin coated pits and raft-dependent pathways (29).

Studies in a number of adherent cell lines have however shown that transferrin internalisation is inhibited (40-60%) in MßCD treated cells (30). Thus the widespread use of MßCD and other cholesterol depleting agents should be cautioned unless control experiments with ligands for clathrin mediated uptake and other pathways are also investigated. Our experiments raise the interesting possibility that the organization of the plasma membrane into cholesterol enriched lipid rafts inhibits plasma membrane translocation. They also suggest that the normal site of entry of the peptides, especially at low temperatures, may be the more fluidic regions of the plasma membrane containing less cholesterol.

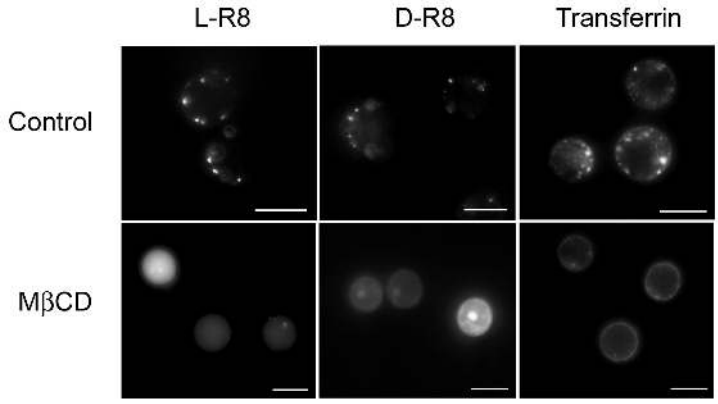

Figure 7. Effect of cholesterol depletion on cellular distribution of R8-Alexa488 peptides and Alexa488-Tf. KG1a cells were pre-incubated in the absence (Control) or presence (MβCD) of 5 mM MβCD for 30 min at 37°C prior to washing and incubation with 2 μM L- or D-R8-Alexa488 or 100 nM Alexa488-Tf for 1 h at 37°C. The cells were then washed and analysed by fluorescent microscopy. Scale bars 10 μm.

At 2 μM concentration, D-R8-Alexa488, unlike L-R8, labeled the nucleolus at all temperatures ≤30˚C, but this was also observed when the peptide concentration was increased 2.5 fold or in plasma membrane cholesterol depleted cells. These are all conditions that showed microscopical evidence for the presence of this peptide in the cytosol, suggesting this is the critical parameter that then allows for sequestration in the nucleolus. At physiological temperatures, proteolysis is likely to contribute much more to L-R8 degradation compared with D-R8 thus the fraction of this peptide that is able migrate to the nucleus and nucleolus is likely to be reduced (8, 31). However we also observe the same differences in localisation when the cells have been pre-cooled to 4˚C and then incubated with the peptides; here protease effects should be significantly diminished. L-R8-Alexa488 is clearly able to translocate to the nucleus at low temperatures, and nuclear, as opposed to nucleolus labeling is often more prominent in L-R8-Alexa488 treated cells (Figure 1). It remains to be seen whether nucleolar sequestration of D-R8 is reducing the extent of the fraction localised to the rest of the nucleus. Nucleolar labeling is a common characteristic of cells that have been incubated with CPPs such as oligoarginine and HIV-TAT and then fixed (7, 32, 33). Our results in unfixed KG1a cells does however support our previous observations of nucleolar labeling of live HeLa cells incubated with the same D-R8 peptide on ice; the extracellular peptide concentration was however appreciably higher at 10 μM (14). An ability to label the nucleolus was also a feature of other CPPs Flu-ß-$(VRR)_4$ and TAT-HA2 (13, 34) suggesting that these also have a propensity to the bind most probably the RNA that is prominent over DNA in these structures.

CONCLUSION

We have analysed in detail the effects of temperature, concentration and peptide chirality on the cellular dynamics of R8 peptide in KG1a cells. Our results suggest that L- and D- forms of the peptides share several similarities such as low temperature translocation but also differences with respect to labeling the nucleolus. Enhancing the fraction of the peptide that localises to the cytosol can be achieved by relatively small increases in peptide concentration or by sequestering plasma membrane cholesterol. These processes seem to be specific for the peptides, as we did not observe any parallel increases in membrane permeability or toxicity. It will now be interesting to investigate whether some of these effects are common to more complex CPPs such as HIV-TAT peptide and penetratin, and also to further determine the capacity of R8 at low temperatures to enhance membrane translocation of associated cargo.

ACKNOWLEDGEMENT

Marjan Fretz is supported by a Marie Curie Host Fellowship for early-stage training in the 6^{th} framework programme of the European Commission. This work was supported in part by Grants-in-Aid for Scientific Research from the Ministry of Education, Culture, Sports, Science and Technology of Japan. Toshihide Takeuchi is grateful for support from the JSPS Research Fellowship for Young Scientists.

REFERENCES

1. S. T. Henriques, M. N. Melo and M. A. Castanho. Cell-penetrating peptides and ant-microbial peptides: how different are they? *Biochem J.* **399:** 1-7 (2006)
2. E. L. Snyder and S. F. Dowdy. Cell-penetrating peptides in drug delivery. *Pharm Res.* **21:** 389-393 (2004)
3. A. H. Joliot and A. Prochiantz. Transduction peptides: from technology to physiology. *Nat Cell Biol.* **6:** 189-196 (2004)
4. S. Deshayes, M. C. Morris, G. Divita and F. Heitz. Cell-penetrating peptides: tools for intracellular delivery of therapeutics. *Cell Mol Life Sci.* **62:** 1839-1849 (2005)
5. K. M. Wagstaff and D. A. Jans. Protein transduction: cell-penetrating peptides and their therapeutic applications. *Curr Med Chem.* **13:** 1371-1387 (2006)
6. M. Lundberg and M. Johansson. Positively charged DNA-binding proteins cause apparent cell membrane translocation. *Biochem Biophys Res Commun.* **291:** 367-71 (2002)
7. J. P. Richard, K. Melikov, E. Vives, C. Ramos, B. Verbeure, M. J. Gait, L. V. Chernomordik and B. Lebleu. Cell-penetrating peptides: A re-evaluation of the mechanism of cellular uptake. *J Biol Chem.* (2002)
8. R. Fischer, K. Kohler, M. Fotin-Mleczek and R. Brock. A stepwise dissection of the intracellular fate of cationic cell-penetrating peptides. *J Biol Chem.* **279:** 12625-12635 (2004)
9. I. M. Kaplan, J. S. Wadia and S. F. Dowdy. Cationic TAT peptide transduction domain enters cells by macropinocytosis. *J Control Release.* **102:** 247-253 (2005)
10. J. P. Richard, K. Melikov, H. Brooks, P. Prevot, B. Lebleu and L. V. Chernomordik. Cellular uptake of unconjugated TAT peptide involves clathrin-dependent endocytosis and heparan sulfate receptors. *J Biol Chem.* **280:** 15300-6 (2005)
11. S. Al-Taei, N. A. Penning, J. C. Simpson, S. Futaki, T. Takeuchi, I. Nakase and A. T. Jones. Intracellular traffic and fate of protein transduction domains HIV-1 TAT and octaarginine, implications for their utilization as drug delivery vectors. *Bioconjug Chem.* **17:** 90-100 (2006)
12. J. R. Maiolo, M. Ferrer and E. A. Ottinger. Effect of cargo molecules on the cellular uptake of arginine-rich cell-penetrating peptides. *Biochem Biophys Acta.* **1712:** 161-72 (2005)
13. G. Tunnemann, R. M. Martin, S. Haupt, C. Patsch, F. Edenhofer and M. C. Cardoso. Cargo-dependent mode of uptake and bioavailability of TAT-containing proteins and peptides in living cells. *Faseb J.* **20:** 1775-84 (2006)
14. I. Nakase, M. Niwa, T. Takeuchi, K. Sonomura, N. Kawabata, Y. Koike, M. Takehashi, S. Tanaka, K. Ueda, J. C. Simpson, A. T. Jones, Y. Sugiura and S. Futaki. Cellular uptake of arginine-rich peptides: roles for macropinocytosis and actin rearrangement. *Mol Ther.* **10:** 1011-22 (2004)
15. P. E. Thoren, D. Persson, P. Isakson, M. Goksor, A. Onfelt and B. Norden. Uptake of analogs of penetratin, Tat(48-60) and oligoarginine in live cells. *Biochem Biophys Res Commun.* **307:** 100-7 (2003)
16. A. Iwasa, H. Akita, I. Khalil, K. Kogure, S. Futaki and H. Harashima. Cellular uptake and subsequent intracellular trafficking of R8-liposomes introduced at low temperature. *Biochem Biophys Acta.* **1758** (2006)
17. S. Afonin, A. Frey, S. Bayerl, D. Fischer, P. Wadhwani, S. Weinkauf and A. S. Ulrich. The cell-penetrating peptide TAT(48-60) induces a non-lamellar phase in DMPC membranes. *Chemphyschem.* **7:** 2134-2142 (2006)
18. C. E. Caesar, E. K. Esbjorner, P. Lincoln and B. Norden. Membrane interactions of cell-penetrating peptides probed by tryptophan fluorescence and dichroism techniques:correlations of structure to cellular uptake. *Biochemistry.* **45:** 7682-7692 (2006)
19. D. Terrone, S. L. Sang, L. Roudaia and J. R. Silvius. Penetratin and related cell-penetrating cationic peptides can translocate across lipid bilayers in the presence of a transbilayer potential. *Biochemistry.* **42** (2003)
20. P. E. Thoren, D. Persson, P. Lincoln and B. Norden. Membrane destabilizing properties of cell-penetrating peptides. *Biophys Chem.* **114:** 169-179 (2005)
21. A. Ziegler, X. L. Blatter, A. Seelig and J. Seelig. Protein transduction domains of HIV-1 and SIV TAT interact with charged lipid vesicles. Binding, mechanism and thermodynamic analysis. *Biochemistry.* **42:** 9185-9194 (2003)
22. T. Mosmann. Rapid colorimetric assay for cellular growth and survival: application of proliferation and cytotoxicity assays. *J Immunol Methods.* **65:** 55-63 (1983)

23. F. R. Maxfield and T. E. McGraw. Endocytic recycling. *Nat Rev Mol Cell Biol.* **5:** 121-132 (2004)
24. E. M. van Dam, T. Ten Broeke, K. Jansen, P. Spijkers and W. Stoorvogel. Endocytosed transferrin receptors recycle via distinct dynamic and phosphatidylinositol 3-kinase-dependent pathways. *J Biol Chem.* **277:** 48876-48883 (2002)
25. D. J. Mitchell, D. T. Kim, L. Steinman, C. G. Fathman and J. B. Rothbard. Polyarginine enters cells more efficiently than other polycationic homopolymers. *J Peptide Res.* **56:** 318-25 (2000)
26. M. Hao, S. Mukherjee, Y. Sun and F. R. Maxfield. Effects of cholesterol depletion and increased lipid unsaturation on the properties of endocytic membranes. *J Biol Chem.* **279:** 14171-14178 (2004)
27. T. Letoha, S. Gaal, C. Somlai, Z. Venkei, H. Glavines, E. Kusz, E. Duda, A. Czajlik, F. Petak and B. Penke. Investigation of penetratin peptides. Part 2. In vitro uptake of penetratin and two of its derivatives. *J Pept Sci.* **11:** 805-811 (2005)
28. E. London. How principles of domain formation in model membranes may explain ambiguities concerning lipid raft formation in cells. *Biochem Biophys Acta.* **1746:** 203-220 (2005)
29. L. Johannes and C. Lamaze. Clathrin-dependent or not: is it still the question? *Traffic.* **3:** 443-451 (2002)
30. S. K. Rodal, G. Skretting, O. Garred, F. Vilhardt, B. Van Deurs and K. Sandvig. Extraction of cholesterol with methyl-beta-cyclodextrin perturbs formation of clathrin-coated endocytic vesicles. *Mol Biol Cell.* **10:** 961-974 (1999)
31. S. T. Gammon, V. M. Villalobos, J. L. Prior, V. Sharma and D. Piwnica-Worms. Quantitative analysis of permeation peptide complexes labeled with Technetium-99m: chiral and sequence-specific effects on net cell uptake. *Bioconjug Chem.* **14:** 368-376 (2003)
32. S. Futaki. Oligoarginine vectors for intracellular delivery: design and cellular uptake mechanisms. *Biopolymers.* **84:** 241-49 (2006)
33. M. Silhol, M. Tyagi, M. Giacca, B. Lebleu and E. Vives. Different mechanisms for cellular internalization of the HIV-1 Tat-derived cell penetrating peptide and recombinant proteins fused to Tat. *Eur J Biochem.* **269:** 494-501 (2002)
34. T. B. Potocky, A. K. Menon and S. H. Gellman. Cytoplasmic and nuclear delivery of a TAT-derived peptide and a beta-peptide after endocytic uptake into HeLa cells. *J Biol Chem.* **278:** 50188-50194 (2003)